ISSN 2079-5459 (print)
ISSN 2413-4295 (online)

UDC 539.216.2: 537.52 doi:10.20998/2413-4295.2020.01.02

REGULARITIES OF THE INFLUENCE OF MICROARC OXIDATION OF ALUMINUM ALLOYS ON THE PHASE-STRUCTURAL STATE OF THE FORMED OXIDE COATINGS AND THE PECULIARITIES OF γ-AL_2O_3 → α-AL_2O_3 POLYMORPHIC TRANSFORMATION DURING THEIR ANNEALING

O. SOBOL', V. SUBBOTINA*

Department of Materials Science, National Technical University "Kharkiv Polytechnic Institute", Kharkiv, UKRAINE
**e-mail: subbotina.valeri@gmail.com*

ABSTRACT *The influence of the technological parameters of microarc oxidation on the regularities of the phase-structural state of coatings formed on D16 aluminum alloys (the main alloying element is Cu) and AMg3 (the main alloying element is Mg) and the effect of annealing in the temperature range 600–1280 °C on the γ-Al_2O_3 → α-Al_2O_3 phase transformation are investigated. It was found that in the coatings formed during microarc oxidation in a complex (alkaline-silicate) electrolyte, three main phase-structural states are revealed: γ-Al_2O_3, α-Al_2O_3 and mullite ($3Al_2O_3 \cdot 2SiO_2$). The conditions of electrolysis allowing the formation of a two-phase state (γ-Al_2O_3 and α-Al_2O_3) on alloys of both types have been determined. It has been established that alloying elements of the AMg3 alloy provide in MAO coatings a higher stability of the γ-$A1_2O_3$ structure in comparison with the analogous state in MAO coatings on D16 alloy. High-temperature annealing of MAO coatings made it possible to reveal a more complete phase transformation on D16 alloy, the structural basis of which is the appearance of tetragonality in the defective cubic lattice of the γ-Al_2O_3 phase. Annealing of MAO coatings stimulates the γ → α transformation with the greatest dynamics of change in the coatings obtained on D16 alloy. At the highest annealing temperature of 1280 °C (for 60 min) as a result of γ→α transformation, the relative content of the α-Al_2O_3 phase in the coating is 89 % (coating obtained on D16 alloy) and 30 % (coating obtained on AMg3 alloy). A model of the polymorphic γ-Al_2O_3 → α-Al_2O_3 transformation in aluminum oxide is proposed, based on the ordering of the metal cationic subsystem in octahedral and tetrahedral internodes and the enhancement of this process upon the weakening of the "metal – oxygen" bond as a result of the replacement of Al ions by Cu ions that have a low binding energy with oxygen. A correlation between the relative content of the α-Al_2O_3 phase and the hardness of the MAO coating was found. With the highest content of the α-Al_2O_3 phase, the hardness reaches 16000 MPa.*
Keywords: *microarc oxidation; aluminum alloy; alkali silicate electrolyte; γ-Al_2O_3; alloying elements; annealing; interstices; tetragonality; polymorphic transformation*

ЗАКОНОМІРНОСТІ ВПЛИВУ МІКРОДУГОВОГО ОКСИДУВАННЯ АЛЮМІНІЄВИХ СПЛАВІВ НА ФАЗОВО-СТРУКТУРНИЙ СТАН ФОРМОВАНИХ ОКСИДНИХ ПОКРИТТІВ І ОСОБЛИВОСТІ γ-Al_2O_3 →α-Al_2O_3 ПОЛІМОРФНОГО ПЕРЕТВОРЕННЯ ПРИ ЇХ ВІДПАЛІ

О. В. СОБОЛЬ, В. В. СУББОТІНА

кафедра матеріалознавства, Національний технічний університет «Харківський політехнічний інститут», м. Харків, УКРАЇНА

АНОТАЦІЯ *Досліджено вплив технологічних параметрів мікродугового оксидування на закономірності фазово-структурного стану покриттів, що формуються на алюмінієвих сплавах Д16 (основний елемент легування Cu) і АМг3 (основний елемент легування Mg) і вплив відпалів в інтервалі температур 600–1280 °С на фазове перетворення γ-Al_2O_3 → α-Al_2O_3. Встановлено, що в покриттях, що формуються при мікродуговому оксидуванні в комплексному (лужно-силікатному) електроліті, виявляються три основні фазово-структурні стани: γ-Al_2O_3, α-Al_2O_3 і мулліт ($3Al_2O_3 \cdot 2SiO_2$). Визначені умови електролізу які дозволяють формуватися двофазному стану (γ-Al_2O_3 і α-Al_2O_3) на сплавах обох типів. Встановлено, що легуючі елементи сплаву АМг3 забезпечують в МДО-покриттях більш високу стабільність структури γ-$A1_2O_3$, в порівнянні з аналогічним станом в МДО-покриттях на сплаві Д16. Високотемпературний відпал МДО-покриттів дозволив виявити повніше фазове перетворення на сплаві Д16 структурною основою якого є поява тетрагональности в дефектної кубічної решітці γ-Al_2O_3 фази. Відпал МДО-покриттів стимулює γ → α перетворення з найбільшою динамікою зміни в покриттях, отриманих на сплаві Д16. При максимальній температурі відпалу 1280 °С (протягом 60 хв.) в результаті γ → α перетворення відносний вміст α-Al_2O_3 фази в покритті становить 89% (покриття, отримане на сплаві Д16) і 30 % (покриття, отримане на сплаві АМг3). Запропоновано модель поліморфного γ-Al_2O_3 → α-Al_2O_3 перетворення в оксиді алюмінію, яка заснована на впорядкування металевої катіонної підсистеми в октаедричних і тетраедричних міжвузлях і посилення цього процесу при ослабленні зв'язку «метал–кисень» в результаті заміщення іонів Al іонами Cu, які мають відносно малу енергію зв'язку з киснем. Виявлено кореляцію між відносним вмістом α-Al_2O_3 фази і твердістю МДО-покриття. При найбільшому вмісті α-Al_2O_3 фази твердість досягає 16000 МПа.*
Ключові слова: *мікродугове оксидування; алюмінієвий сплав; лужно силікатний електроліт; γ-Al_2O_3; елементи легування; відпал; міжвузля; тетрагональність; поліморфне перетворення.*

Introduction

Despite the fact that the theoretical concepts of the nature of the phenomena on which the technology of microarc oxidation of aluminum coatings is based are still far from perfect, very effective methods of producing

coatings with different properties have been developed empirically [1–3].

However, further development of this technology requires a more in-depth knowledge of the processes occurring during the formation of MAO coatings, which makes it possible to purposefully change the oxidation conditions in order to obtain the required coating characteristics [4–6]. In this aspect, the study of the influence of the elemental composition of the alloy on the phase composition of the formed coating and the features of the γ-$Al_2O_3 \rightarrow \alpha$-$Al_2O_3$ polymorphic transformation during the formation of MAO coatings on aluminum alloys is undoubtedly of interest, since these phases are the main phases in MAO coatings and determine their properties [7,8].

The purpose of the work

Therefore, the aim of this work was to establish the effect of microarc oxidation in complex electrolytes of different composition on the phase composition and properties of D16 (the main alloying element is Cu) and AMg3 (the main alloying element is Mg) alloys, as well as the effect on the phase-structural state of these coatings by annealing in temperature range of 600–1280 °C.

Literature review

The polymorphic modification of α-Al_2O_3 aluminum oxide has a rhombohedral crystal lattice (a = 0,512 nm, α = 55,25°, for a hexagonal setting a = 0,475 nm, c = 1,299 nm, space group D^6_{3d}). The crystal lattice of α-Al_2O has significant stability and strength; therefore, corundum recrystallization requires very high temperatures (about 1800–1900 °C). During recrystallization in the solid phase for the development of exchange processes or self-diffusion, it is necessary to overcome a significant energy barrier [9]. The structure of the α-$A1_2O_3$ oxide is built on the basis of dense filling of the anionic lattice and various possibilities of filling octahedral and tetrahedral interstices with cations. In the α-$A1_2O_3$ lattice 2/3 of octahedral interstices are occupied, as a result of which, due to the strong electrostatic attraction between aluminum cations and oxygen anions, as well as close packing, the formation of solid solutions is difficult.

The structure of γ-Al_2O_3 is traditionally considered as a type of spinel with defects, in which oxygen atoms are located in a cubic close packing, and Al atoms occupy octahedral and tetrahedral positions. However, unlike fully occupied positions in the oxygen sublattice, the aluminum sublattice contains structural vacancies that balance the [Al]/[O] ratio. In the $Fd\bar{3}m$ space group, this means that oxygen is in the positions of fcc lattice sites, and Al atoms are in tetrahedral and octahedral positions. To satisfy the stoichiometry of γ-Al_2O_3, in contrast to the chemical formula of spinel, M_3O_4 (M = metal or mixture of metals), the atomic positions of Al are not fully occupied. Vacancies are distributed by both tetrahedral and octahedral positions. However, until now the exact distribution of Al atoms (and vacancies) has been controversial [10], and apparently depends on the conditions for obtaining γ-Al_2O_3 [11].

During the formation of intermediate phases of aluminum oxide, these vacancies show different degrees of ordering, which usually increases from γ-Al_2O_3 to θ-Al_2O_3 [12]. Different distribution of vacancies over cation sites: one of the reasons why different structural descriptions of γ-Al_2O_3 can be found in the literature for samples obtained by different technologies, with different crystallite sizes, etc. [13,14].

The γ-Al_2O_3 phase has a much lower surface energy and higher entropy, and therefore can be more stable at low temperatures [15]. As shown by calculations [16], the value of the free surface energy of the γ-Al_2O_3 phase is 1,7 J/m^2, and for the α-Al_2O_3 phase the value of the surface energy is 2.6 J/m^2.

At temperatures exceeding 1200 °C, γ-Al_2O_3 transforms into α-Al_2O_3 [17].

Therefore, it is generally accepted that the heat resistance of MAO coatings is about 1200 °C. However, the fact that the properties of MAO coatings are determined not only by the quantitative ratio of the α-Al_2O_3 and γ-$A1_2O_3$ phases suggests that during heating at temperatures below 1200 °C, changes in the structure of these phases are possible. It should be noted that the transformation temperature can change in magnitude upon aluminum alloying [18].

Thus, as follows from the literature review, the issues related to the regularities of the formation of the γ-$A1_2O_3$ phase and the degree of its stability during the formation of MAO coatings on alloys of different compositions remain debatable; there is no generally recognized mechanism of γ-$Al_2O_3 \rightarrow \alpha$-$Al_2O_3$ polymorphic transformation and the influence of the conditions of plasma treatment and thermal annealing. All this is the basis of the structural-phase engineering of MAO coatings and determines their functional properties.

Microarc oxidation and research methodology

Microarc oxidation was carried out in a 100 liter stainless steel bath. During the MAO process, cooling and bubbling of the electrolyte was provided. The average voltage was 380 V. The current density was 20 A/dm^2.

Based on the results of preliminary studies, D16 and AMg3 aluminum alloys were used as model alloys for microarc oxidation, since at close parameters of MAO treatment, a coating of approximately the same thickness on these alloys, consisting only of γ-$A1_2O_3$ and α-Al_2O_3 phases is formed, but with a significant difference in their ratio. In addition, an important difference between these alloys was the main alloying element: in D16 such an element is Cu, which has a very weak bond with oxygen, and in AMg3 such an element is Mg, which has a relatively high binding energy with oxygen in oxides and belongs to valve elements group [19].

ISSN 2079-5459 (print)
ISSN 2413-4295 (online)

In this case, the composition of the D16 alloy as the main elements includes: Al (90,9–94,7 %), Cu (3,8–4,9 %), Mg (1,2–1,8 %), Mn – in the range of 0,3–0,9 %, Fe – no more than 0,5 %; Si – no more than 0,5 %; Zn – up to 0,25 %; Ti – no more than 0,15 %), and in the AMg3 alloy, the main elements are: Al (93,8–96 %), Mg – (3,2–3,8 %), Mn – (0,3–0,6 %), Si – (0,5–0,8 %), Ti – up to 0,1 %, Fe – up to 0,5 %.

The process of microarc oxidation was carried out in an alkali-silicate electrolyte at an initial pH = 10,0–13,0 and ρ = 100–350 Ohm/cm. However, to obtain a high-quality oxide coating on these alloys, a final adjustment of pH and ρ was necessary. The electrolytes and MAO modes used to optimize the technology of coating deposition on D16 and AMg3 alloys are given in tabl. 1.

Table 1 – Types and characteristics of electrolytes used for microarc oxidation

No	Electrolyte composition, g/L		pH	ρ, Ohm/cm
	KOH	Na_2SiO_3		
1	1	6	11,60	254
2	2	12	11,90	150
3	2	6	12,4	130

To clarify the nature of the processes that led to a change in the lattice period of the γ-$A1_2O_3$ phase, MAO coatings on D16 and AMg3 alloys were separated. The separation of the MAO coating was carried out by dissolving the aluminum base with exposure in an 18 % hydrochloric acid solution for 20–30 minutes (until the aluminum base is completely dissolved). The absence of an aluminum base was monitored by diffraction spectra.

The separated coatings were annealed for 60 minutes at temperatures of 600, 700, 800, 900, 1000, 1100, 1120, 1280 °C.

After exposure to each temperature the phase composition of the coatings and the lattice period of the γ-$A1_2O_3$ and α-Al_2O_3 phases were studied by X-ray diffractometry.

X-ray diffraction studies were carried out on a DRON-3 X-ray diffractometer with point-to-point recording of diffraction reflections. To determine the lattice parameters of the γ-$A1_2O_3$ and α-Al_2O_3 phases, the survey was carried out in λ-Cr radiation with a V filter. The phase concentration was determined using reference points for each of the possible phases. The scanning was carried out in a pointwise mode with a Δ (2θ) = 0.02° scanning step and a pulse accumulation time at each point of 20 s. For complex diffraction profiles, they were decomposed with the selection of the component peaks. Decomposition was carried out using the «new_profile 3.4» software package [20]. To interpret the diffraction patterns, the tables of the International Center for Diffraction Data (Powder Diffraction File [21]) were used.

Scanning electron microscopic analysis of surface morphology was performed on the REM MA 101.

Microhardness was determined using a PMT-3 device.

Results

Oxidation was carried out for 1 hour, when it is believed that the thickness of the dielectric layer in the microplasma channels does not yet lead to a significant enrichment of the crystalline lattice of the γ-$A1_2O_3$ phase with impurity atoms of the alloy [19]. In this case, the lattice period of γ-$A1_2O_3$ should be close to the standard values for the γ-$A1_2O_33$ phase of 0.7917–0.792 nm.

Fig. 1 shows comparative histograms of compositions of MAO coatings on D16 and AMg3 alloys obtained in different electrolytes.

It can be seen that when using electrolytes of the first 2 types (tabl. 1), mullite is present as one of the phases in the coating composition. Therefore, such electrolytes cannot be used to obtain only the basic α-Al_2O_3 and γ-$A1_2O_3$ phases and at the same time achieve a high-hardness state (with a hardness of more than 15 000 MPa).

Fig. 2 shows the dependence of the hardness of MAO coatings on the composition of the electrolyte.

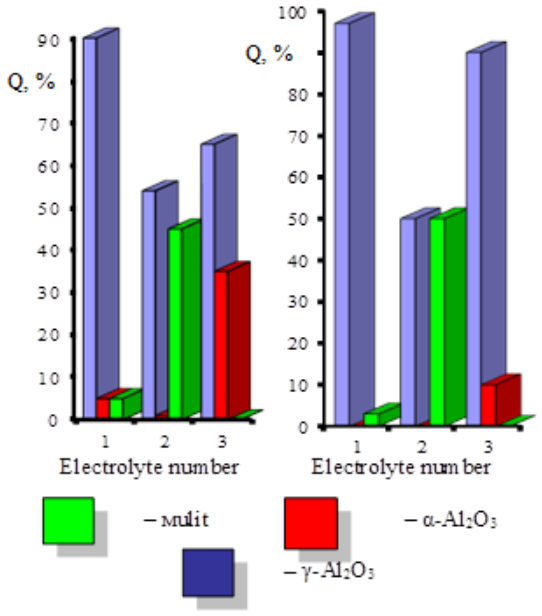

a – D16 b – AMg3

Fig. 1 – Phase composition of MAO coatings on the D16 (a) and AMg3 (b) alloys in electrolytes of different types (τ = 1 hour)

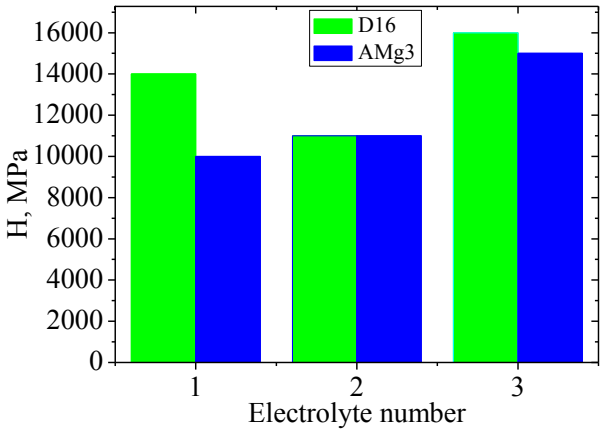

Fig. 2 – Dependence of the hardness of MAO coatings on the electrolyte composition (electrolyte number in accordance with tabl. 1)

As can be seen from the results presented in fig. 2, the highest hardness is inherent in MAO coatings formed during electrolysis in the 3rd electrolyte. In this case, under the same electrolysis conditions, the hardness of MAO coatings on D16 alloy turned out to be higher than in coatings on AMg3 alloy. If we compare the data on hardness and phase composition (fig. 1), we can trace the relationship between the amount of α-Al_2O_3 in the coating composition and the hardness of the coating (with an increase in the relative content of α-Al_2O_3 in the coating, its hardness increases).

Also, when analyzing the results obtained, it can be seen that the same hardness is not always realized with the same phase composition. Obviously, in addition to a change in the phase composition, there is also a change in the structural characteristics of the phases themselves.

Based on the results presented in Fig. 1 and fig. 2, coatings obtained after MAO treatment of D16 and AMg3 alloys in electrolyte 3 (2 g/L KOH + 6 g/L Na_2SiO_3 solution) were selected for basic studies. The thickness of such coatings was about 80 μm, and the phase composition included only γ-$A1_2O_3$ and α-Al_2O_3 phases.

Fig. 3 shows the morphology of the lateral surface of such a coating on the AMg3 alloy. It is seen that the coating has a fairly uniform structure with low porosity.

Separated MAO coatings were obtained by dissolving the base of the aluminum alloy in an 18 % hydrochloric acid solution.

It should be noted that the same hardness is not always realized with the same phase composition. Obviously, in addition to a change in the phase composition, there is also a change in the structural characteristics of the phases themselves. Therefore, in the work, both the phase composition and the lattice period of the base α-Al_2O_3 and γ-$A1_2O_3$ phases were studied.

To analyze the phase composition, reference lines of α-Al_2O_3 and γ-$A1_2O_3$ phases were used. As such lines (113) were chosen for α-Al_2O_3 and (400) for γ-$A1_2O_3$. These peaks have a fairly high relative intensity and are located in a close angular range.

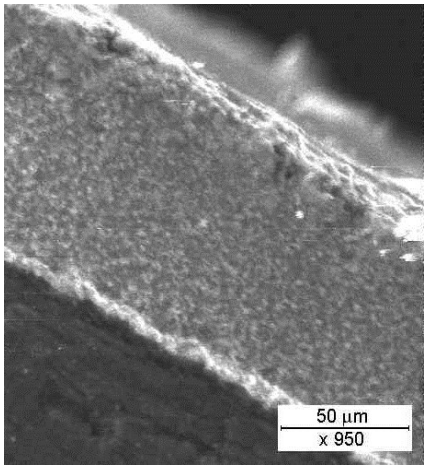

Fig. 3 – Morphology of MAO coating on D16 alloy

Fig. 4 and fig. 5 show the resulting dependences of the relative content of α-Al_2O_3 and γ-$A1_2O_3$ phases in the coating on the annealing temperature.

It can be seen that the phase composition remains practically unchanged up to a temperature of about 800 °C. Significant changes in the composition occur at temperatures exceeding 900 °C. In this case, to the greatest extent, this applies to D16 alloy (fig. 4).

Thus, a change in the composition of coatings at high temperatures due to an increase in the relative content of the α-$A1_2O_3$ phase indicates the stimulation of the γ-$A1_2O_3$ → α-Al_2O_3 phase transition at these temperatures. An important structural indicator of such a transition is the lattice period.

The lattice period of γ-$A1_2O_3$ in the separated MAO coating on the D16 alloy was 0,7917 nm, and in the coating on the AMg3 alloy, the lattice period of the γ-$A1_2O_3$ phase was 0,7915 nm.

To determine the effect of annealing temperature at high temperatures, a precision measurement of the lattice period of the γ-$A1_2O_3$ phase was carried out during annealing in a wide temperature range.

From the sections of the diffraction spectra presented in fig 6 and fig. 7, after their decomposition into component profiles, it can be seen that at temperatures up to 900 °C, two diffraction peaks from the (440) planes of the γ-$A1_2O_3$ phase and (124) α-Al_2O_3 phase are revealed. It should be noted that the (440) diffraction line is symmetrical. An increase in the annealing temperature above 900 °C leads to a shift of the diffraction peak from the (440) γ-$A1_2O_3$ planes to the region of large diffraction angles (which corresponds to a decrease in the period) and the appearance of an additional peak in a smaller angular range.

To determine the lattice parameters of the γ-$A1_2O_3$ phase, the survey was carried out in λ-Cr radiation at large angles (in the angular range 2θ = 108–111°) with a scanning step of 0,010. This made it possible to determine the shape and position of the most intense reflection in this range of large angles from the (440) plane of the γ-$A1_2O_3$ phase.

ISSN 2079-5459 (print)
ISSN 2413-4295 (online)

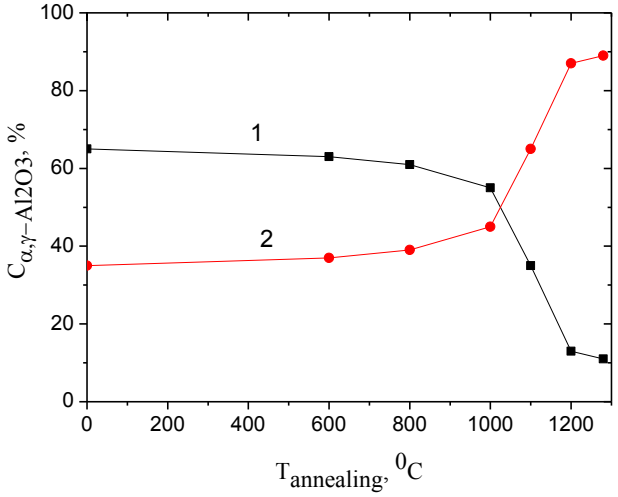

Fig. 4. – Phase composition of MAO coatings on D16 alloy after their annealing: 1 – γ-$A1_2O_3$, 2 – α-Al_2O_3

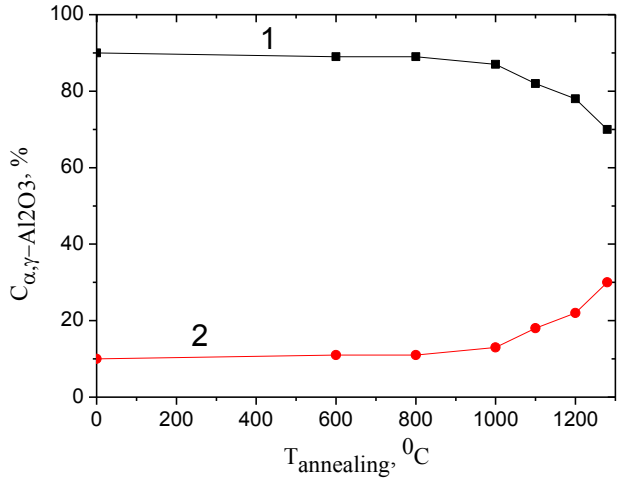

Fig. 5 – Phase composition of MAO coatings on the AMg3 alloy after their annealing: 1 – γ-$A1_2O_3$, 2 – α-Al_2O_3

It was found that up to a temperature of about 900 °C the lattice period remains practically unchanged and close to 0,7916 nm, which is consistent with the microstructural data for γ-$A1_2O_3$.

Fig 6 and fig. 7 show a typical view of the spectral regions in the selected angular range.

It should be noted that in this case, the position of the (124) peak of the α-Al_2O_3 phase practically does not change. Precision measurements of the lattice period of α-Al_2O_3 in coatings in the entire temperature range of annealing (600–1280 °C) did not reveal its change, which indicates the stability of the corundum lattice. Thus, in contrast to γ-$A1_2O_3$, the period of the rhombic lattice of α-$A1_2O_3$ is practically constant (a = 0,5127 + – 0,0002 nm, α = 55,280).

In γ-$A1_2O_3$, the (440) diffraction peak is divided into two components with an intensity ratio close to 1:2. The appearance of an additional diffraction peak with a simultaneous shift of the basic peak to the region of large angles has signs of the appearance of tetragonality in the cubic lattice of the γ-$A1_2O_3$ phase.

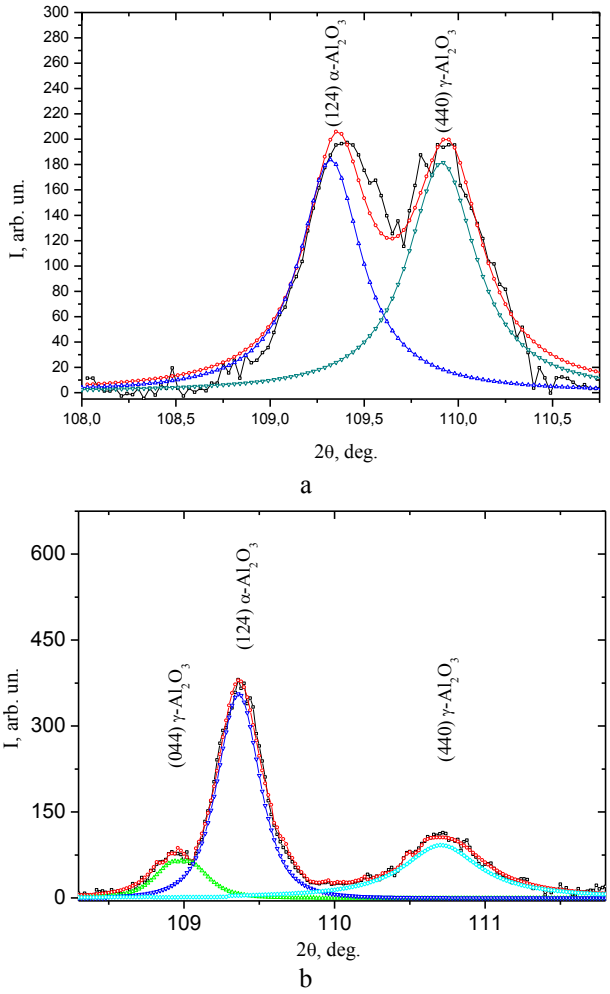

Fig. 6 – X-ray diffraction patterns (with decomposition into components) of MAO coatings obtained on D16 alloy after annealing for 60 minutes at a temperature of 800 °C (a) and 1280 °C (b)

Based on this approach, Fig. 8 shows the change in the interplanar distance of γ-$A1_2O_3$ for planes of the (440) type and its separation into 2 components (440) and (044) at high temperatures.

The obtained values of the change in the interplanar spacing indicate the appearance of anisomericity of the periods, which indicates that the lattice passes from cubic to tetragonal with a degree of tetragonality c/a ≈ 1.02. The temperature of such a transition for the coating on D16 and AMg3 alloys is slightly different. As can be seen from the results obtained, the appearance of such a doublet of peaks is clearly revealed on MAO coatings of the D16 alloy at 1000 °C (fig. 8a). At the same time, on the MAO coatings of the AMg3 alloy, a noticeable appearance of the tetragonality doublet manifests itself only at temperatures above 1100 °C (fig. 8b).

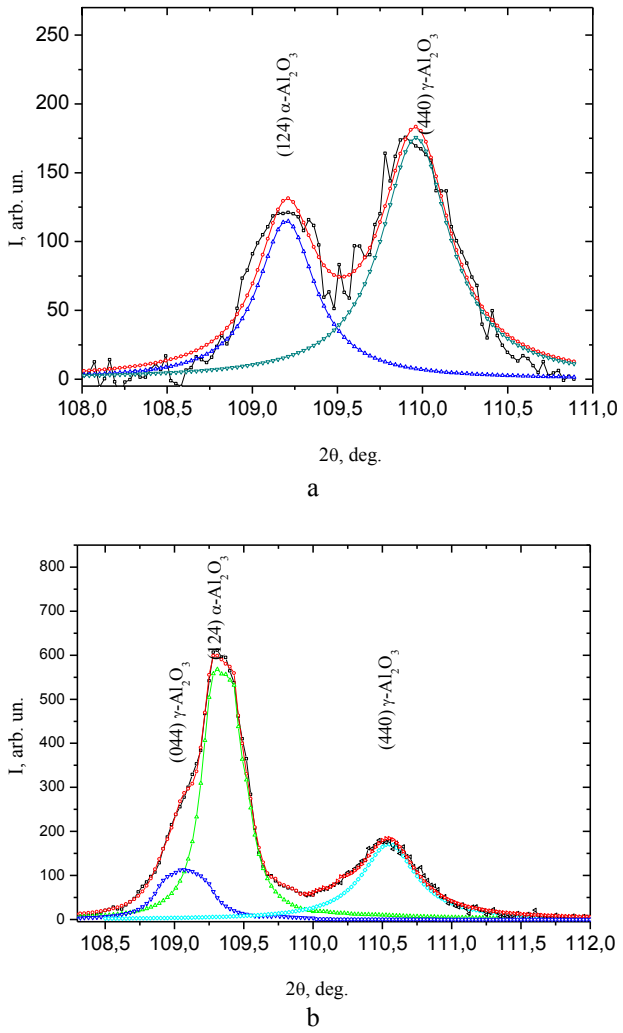

Fig. 7 – X-ray diffraction patterns (with decomposition into components) of MAO coatings obtained on the AMg3 alloy after annealing for 60 minutes at a temperature of 800 °C (a) and 1280 °C (b)

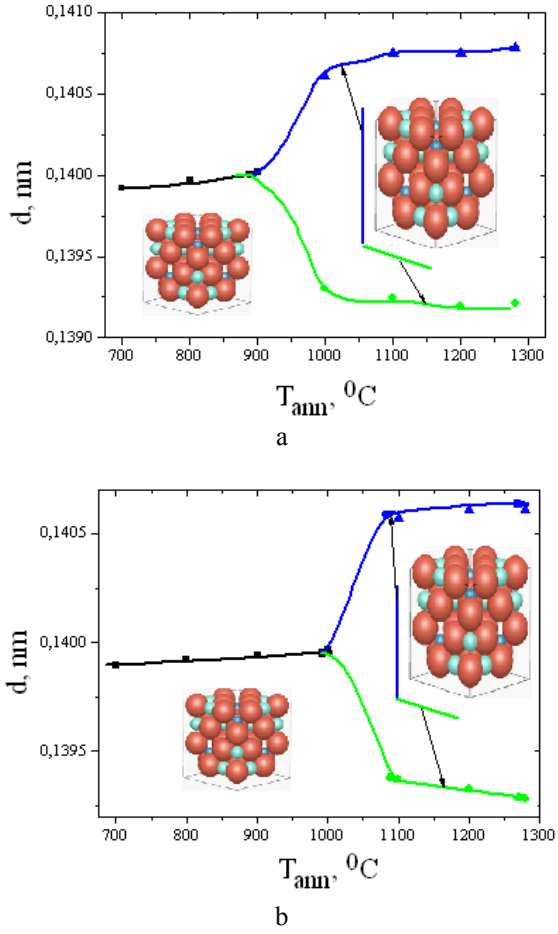

Fig. 8 – Change in the interplanar spacing for the (440) plane of the γ-Al_2O_3 phase with the formation of tetragonality in the lattice of the coating formed on the D16 (a) and AMg3 alloys upon their annealing

Discussion of results

It is known [19] that in the composition of films obtained by conventional anodizing of aluminum alloys, α-Al_2O_3, the γ-Al_2O_3 → α-Al_2O_3 transition is not detected, since the process temperature is lower than 1000 °C.

With MAO, the temperature in the discharge channels can reach 3000 °C and higher temperatures [19]. However, apparently, due to the high dispersion at the initial formation of the phase from the plasma, at the initial stage of oxidation, the γ-Al_2O_3 phase is mainly formed. The formation of an amorphous or nanocrystalline γ-Al_2O_3 phase during the MAO process is determined by a high degree of nonequilibrium of the processes during microplasma oxidation at which the highly dispersed form of γ-Al_2O_3 is more stable than α-Al_2O_3 due to the lower surface energy [22].

In addition, the stabilization of the γ-Al_2O_3 phase is facilitated by the partial replacement of the ionic component at the lattice sites with ions such as Na^+, K^+ and ions of other metals. Therefore, the different chemical nature of the stabilizer ions of the γ-Al_2O_3 phase during the oxidation of different alloys explains the difference in the γ-Al_2O_3 → α-Al_2O_3 transition temperature.

It should be noted that with an increase in the duration of the process, there is a change in the power of microarc discharges and the temperature in the microarc zone, that is, the transformation temperature, and it can be assumed that in this case the processes of redistribution of ions (their type and ratio is determined by the chemical composition of the alloy and electrolyte) into the composition of γ-Al_2O_3, as well as to undergo ordering in the crystal lattice, which cause a change in its lattice parameter.

The results obtained indicate that at high temperatures ordering occurs in the γ-Al_2O_3 lattice with the formation of tetragonality.

It is known that the γ-Al_2O_3 phase is metastable and is mainly detected with a cubic type unit cell [23]. However, in a number of works, the possibility of the

ISSN 2079-5459 (print)
ISSN 2413-4295 (online)

appearance of tetragonality in such a lattice was noted [24,25]. In this case, the stabilization of the cubic lattice occurs upon separation from the nanocrystalline and amorphous structure [26,27]. This is determined by the relatively low surface free energy [14]. Therefore, with an increase in temperature and an increase in the grain structure, the stability of γ-$A1_2O_3$ decreases.

The cubic crystal cell of γ-$A1_2O_3$ belongs to the spinel structure. In the spinel structure ($Me^{2+}Me_2^{3+}O_4$), the unit cell includes 32 O anions, which form the densest cubic packing with 64 tetrahedral (cations occupy 8) and 32 octahedral (cations occupy 16) vacancies. In such vacancies, there should be 24 metal ions. The unit cell of γ-Al_2O_3 contains 32 oxygen ions (i.e., the anionic part corresponds to the filling for classical spinel), however, the cationic part accounts for 21 1/3 of the metal ion (that is, it contains 8 $A1_2O_3$ molecules). This is due to the fact that in γ-Al_2O_3 the Al^{3+} ion plays the role of both Me^{2+} and Me^{3+} cations. Al^{3+} ions are statistically distributed over 8 tetrahedral and 16 octahedral positions. Therefore, the structure of γ-$A1_2O_3$ is called a defect-type spinel structure, and upon exposure to temperature, a redistribution of Al^{3+} ions over octahedral and tetrahedral positions can occur, which affects the lattice period.

This model is described more fully in [28]. In this case, the traditional structure model is used, such as a defective cubic spinel of the AB_2O_4 formula, where A = B = Al and in which A atoms occupy 1/8 tetrahedral positions (interstitial sites), B atoms occupy 1/2 octahedral positions (interstitial sites). This structure is shown in Fig. 9.

However, as the works of recent years [29] have shown, the used model of the structure of γ-Al_2O_3, in which 25% of Al^{3+} cations are located in tetrahedral interstices and tetrahedral interstices are the main vacancies for aluminum ions, must be modified. This is due to the fact that, as shown by NMR studies, a significant part of vacancies can be in octahedral interstices, as in isostructural γ-Fe_2O_3. In this case, two Al vacancies in octahedral interstices maximize their distances [30–35].

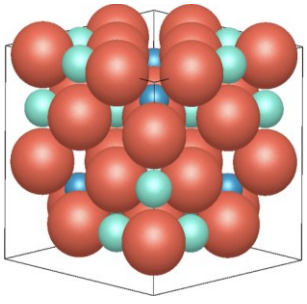

Fig. 9 – Structure of AB_2O_4 spinel. The large red spheres are O atoms at the sites of the fcc lattice, the small blue spheres are the A atoms at the tetrahedral interstices, and the green small spheres are the B atoms at the octahedral interstices

In this case, as is known [36], in the presence of more than 20 % of vacancies in a cubic (with a base of the fcc type) sublattice, their ordering occurs with increasing temperature. The degree of such ordering is influenced by the bond strength between metal and non-metal ions (in this case, oxygen).

In this case, the distortions of the crystalline lattice of the γ-Al_2O_3 spinel can mainly be associated with displacements of oxygen ions, which lead to «rotations» of the AlO_6 octahedra. And in the case of atomic ordering and the appearance of tetragonality of the lattice, alternation of layers consisting of aluminum octahedra with layers consisting of aluminum octahedra and tetrahedra should be observed.

If we compare these 2 crystalline lattices, then α-$A1_2O_3$ has a structure with the oxygen planes ABAB along the z axis. On the other hand, γ- $A1_2O_3$ has a cubic structure (Fd-3m groups) based on an fcc lattice with the oxygen planes ABCABC along the z axis. Unlike α-$A1_2O_3$, it has free spaces in Al positions. And unlike α-$A1_2O_3$, which occupies 2/3 of the octahedral positions of the insertion, γ- $A1_2O_3$ occupies not only the octahedral position, but also tetrahedral positions. A schematic view of close-packed planes for these types of lattices is shown in Fig. 10 [37].

Thus, the transition from the γ-$A1_2O_3$ structural state to α-$A1_2O_3$ can occur by a shear path, which requires a transformation of the rhombohedral unit cell. One of the stages of such a transition is the change of the rhombic cell inscribed into the cubic lattice of γ-$A1_2O_3$ to the required parameters in the hexagonal setting of the α-$A1_2O_3$ phase. Such a change should take place through the tetragonality stage, as shown in Fig. 11.

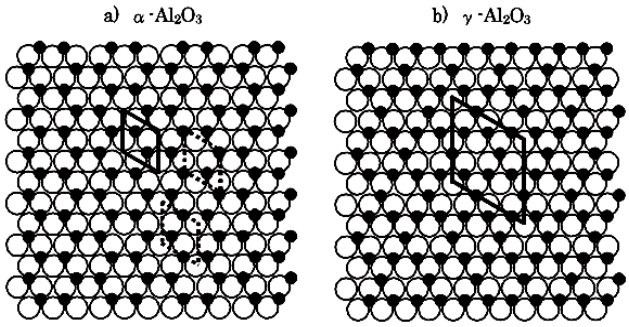

Fig. 10 – Model structures of α-$A1_2O_3$, (0001) plane and γ-$A1_2O_3$, (111) plane. Rhombuses in the structures show the unit cell (white – oxygen anions, black – aluminum cations) [37]

It should be should be considered that during MAO treatment of alloys containing several elements, isovalent isomorphism is absent, that is, when the ions replacing each other have the same valence, and heterovalent isomorphism is realized, when the ions replacing the initial one have a different valence. In addition, the alloying metal ions replacing Al^{3+} differ in their ionic radius. For the studied alloys, the Al^{3+} cation has an ionic radius of 0,067 nm, Cu^{2+} (0,087 nm), Cu^{3+}

(0,068 nm), Mg^{2+} (0,086 nm), and the O^{-2} anion (0,126 nm). In this case, it is necessary that the lattice as a whole be neutral, that is, for the compensation of valence (charge) to occur. Vacancies can play the role of charge compensators.

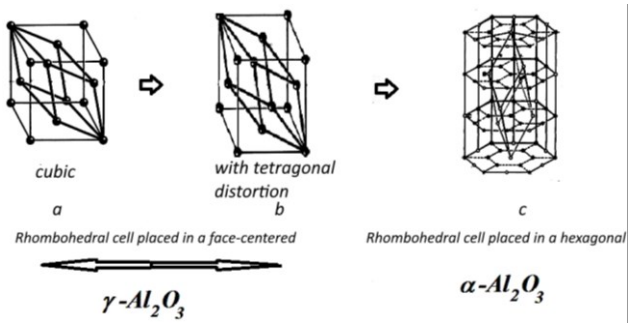

Fig. 11 – Scheme of rhombohedral cell transformation from a cubic (fcc) γ-$A1_2O_3$ setting (a), through a tetragonally distorted γ-$A1_2O_3$ lattice (b) to a hexagonal α-$A1_2O_3$ phase setting (c)

Compensation can occur not only for the positions of ions occupying the same sublattice, but also for the positions of different systems. The appearance of vacancies that compensate for the charge during the formation of solid solutions in crystals is accompanied by an increase in the lattice period. Apparently, the formation of defect structures can explain an increase in the lattice period of the γ-$A1_2O_3$ phase during the formation of coatings on the alloys under study. In addition, the difference in ionic radii also leads to a change in the period.

Since an increase in the oxidation time leads to an increase in the thickness of the dielectric layer, during the MAO process the discharge power increases (the temperature in the discharge channels increases) and the degree of doping of the formed MAO coating with impurity ions increases. Therefore, the observed increase in the period of γ-$A1_2O_3$ can be associated both with an increase in the content of cations with a larger atomic radius, and with the appearance of compensating vacancies.

In contrast to this, an increase in the γ-$A1_2O_3$ period upon annealing of a coating with a temperature of 600 – 900 °C can be associated only with the appearance of compensating vacancies or rearrangement in the lattice for the transition to a more thermodynamically equilibrium state of α- $A1_2O_3$. Taking into account the short duration of exposure to microarc discharges (microseconds) at high temperatures (about 3000 °C), which is several times higher than the γ → α transformation temperature, it can be assumed that the ordering processes during MAO processing occur much more intensively, which complicates the fixation of this transformation stage. γ → α (formation of tetragonality) in the MAO process.

In the case of prolonged annealing at relatively low temperatures, as was done in this work, the stage of tetragonal distortions appeared during the transition of the nonequilibrium γ-$A1_2O_3$ phase to the equilibrium close-packed α-$A1_2O_3$ phase (Fig. 7 and Fig. 8).

The different kinetics of such transformations in the D16 alloy (where the main alloying element is Cu) in comparison with the AMg3 alloy (where the main alloying element is Mg) can be explained in the model of the defect structure of γ-$A1_2O_3$ crystal lattice, as the driving force of the polymorphic transformation into thermodynamically stable α-$A1_2O_3$ phase.

In the absence of impurity ions, such a transition becomes possible when the Al^{3+}/O^{2-} bond weakens upon reaching a high temperature (more than 1200 °C), which provides the necessary diffusion mobility for the γ → α transformation. This transformation is initially thermodynamically favorable due to the presence of vacancy defects in the Al cation sublattice of the γ-$A1_2O_3$ phase. In the case of alloying with magnesium (AMg3 alloy), which also has a relatively large bond strength with oxygen (according to [12], the free energy of formation of aluminum oxide is about 1100 kJ/mol, and for magnesium oxide, about 1160 kJ/mol), its substitution in the Al^{3+} cation sublattice does not lead to a significant change in the kinetics of the γ → α transformation.

In contrast to the AMg3 alloy in the D16 alloy, Cu is the main degassing element. Copper has a very low oxide formation energy (about 300 kJ/mol [19]), which determines a relatively weak bond between oxygen and copper in the lattice. Therefore, when alloying with Cu, the replacement of Al^{3+} cations with Cu^{3+} (or Cu^{2+}) leads to a weakening of the bond with oxygen in the lattice, which makes it possible to increase the kinetics of the diffusion-shear transformation into the α-$A1_2O_3$ phase.

Thus, the above study allows us to state that the γ-$A1_2O_3$ phase is characterized by different degrees of ordering, and hence properties, as well as different tendencies to γ-$A1_2O_3$ → α-$A1_2O_3$ transformation.

Based on this approach, it can be recommended to use metals with a low free energy of oxide formation as alloying elements to increase the kinetics of γ → α transformation during microarc oxidation of aluminum alloys, which include Cu, Ni, Fe, and W.

Also, taking into account the results of an increase in the degree of γ-$A1_2O_3$ → α-$A1_2O_3$ transformation during high-temperature annealing, it can be recommended to increase the relative content of the α-$A1_2O_3$ phase in MAO coatings on the AMg3 alloy, which determines an increase in the performance characteristics of products made of this alloy with MAO coatings, use the modes of the MAO process leading to an increase in the duration of the pulse.

Conclusions

By the method of microarc oxidation of D16 and AMg3 aluminum alloys, oxide coatings the composition of which includes γ-Al_2O_3, α-Al_2O_3 and mullite ($3Al_2O_3 \cdot 2SiO_2$) were obtained.

A correlation between the relative content of the α-Al_2O_3 phase and the hardness of the MAO coating was

ISSN 2079-5459 (print)
ISSN 2413-4295 (online)

found. With the highest content of the α-Al_2O_3 phase (35%), the hardness reaches 16000 MPa.

It has been determined that coatings with a thickness of about 80 μm, the phase composition of which includes only γ-Al_2O_3 and α-Al_2O_3, can be obtained on both types of alloys by electrolysis in an electrolyte with a composition of 2 g/L KOH + 6 g/L Na_2SiO_3.

It has been established that alloying elements of the AMg3 alloy provide in MAO coatings a higher stability of the γ-$A1_2O_3$ structure in comparison with the analogous state in MAO coatings on D16 alloy.

Annealing of MAO coatings stimulates the γ → α transformation with the greatest dynamics of change in the coatings obtained on D16 alloy. At the highest annealing temperature of 1280 °C (for 60 min) as a result of γ→α transformation, the relative content of the α-Al_2O_3 phase in the coating is 89 % (coating obtained on D16 alloy) and 30 % (coating obtained on AMg3 alloy).

The effect of displacement of diffraction peaks and the formation of subpeaks at annealing temperatures of MAO coatings of more than 1000 °C are revealed, which is typical for the appearance of tetragonality in the cubic lattice of γ-Al_2O_3 with a spinel structure.

A model of the polymorphic γ-Al_2O_3 → α-Al_2O_3 transformation in aluminum oxide is proposed based on the ordering of the metal cationic subsystem in octahedral and tetrahedral interstices and the enhancement of this process upon the weakening of the «metal–oxygen» bond as a result of the replacement of Al ions by Cu ions having low binding energy with oxygen.

Список літератури

1. Xiang N., Song R.-g., Zhuang J.-j. Song R.-x., Lu X.-y., Su X.-p. Effects of current density on microstructure and properties of plasma electrolytic oxidation ceramic coatings formed on 6063 aluminum alloy. *Transactions of nonferrous metals society of china*. 2016. 26. Iss. 3. P. 806–813. doi: 10.1016/S1003-6326(16)64171-7.
2. Kharanagh V. J., Sani M. AF., Rafizadeh E. Effect of current frequency on coating properties formed on aluminized steel by plasma electrolytic oxidation. *Surface engineering*. 2014. 30. Iss. 3. P. 224–228. doi: 10.1179/1743294413Y.0000000190.
3. Martin J., Melhem A., Shchedrina I., Duchanoy T., Nominé A., Henrion G., Czerwiec T., Belmonte T. Effects of electrical parameters on plasma electrolytic oxidation of aluminium. *Surface and coatings technology*. 2013. 221. P. 70–76. doi: 10.1016/j.surfcoat.2013.01.029.
4. Lesnevskiy L. N., Lyakhovetskiy M. A., Ivanova S. V., Nagovitsyna O. A. Structure and properties of surface layers formed on zirconium alloy by microarc oxidation. *Journal of surface investigation. X-ray, synchrotron and neutron techniques*. 2016. 10. Iss. 3. P. 641–647. doi: 10.1134/S1027451016030289.
5. Li H. X., Li W. J., Song R. G., Ji Z. Effects of different current densities on properties of MAO coatings embedded with and without a-Al_2O_3 nanoadditives. *Materials science and technology*. 2012. 28. Iss. 5. P. 565–568. doi: 10.1179/1743284711Y.0000000084.
6. Veys-Renaux D., Rocca E., Henrion G. Micro-arc oxidation of AZ91 Mg alloy: An in-situ electrochemical study. *Electrochemistry communications*. 2013. 31. P. 42–45. doi: 10.1016/j.elecom.2013.02.023.
7. Subbotina V., Al-Qawabeha U. F., Belozerov V., Sobol' O., Subbotin A., Tabaza T. A., Al-Qawabah S. M. Determination of influence of electrolyte composition and impurities on the content of α-Al_2O_3 phase in mao-coatings on aluminum. *Eastern-European journal of enterprise technologies*. 2019. 6. Iss. 12 (102). P. 6–13. doi: 10.15587/1729-4061.2019.185674.
8. Belozerov V., Mahatilova A., Sobol' O., Subbotina V., Subbotin A. Investigation of the influence of technological conditions of microarc oxidation of magnesium alloys on their structural state and mechanical properties. *Eastern-European journal of enterprise technologies*. 2017. 2. Iss. 5 (86). P. 39–43. doi: 10.15587/1729-4061.2017.96721.
9. Брон В. А. О рекристаллизации корунда. Доклады Академии Наук СССР. 1951. Т. 80. № 4. С. 661–664.
10. Tsybulya S. V., Kryukova G. N. Nanocrystalline transition aluminas: Nanostructure and features of x-ray powder diffraction patterns of low-temperature Al_2O_3 polymorphs. *Physical Review B*. 2008. 77. Iss. 2. P. 024112. doi: 10.1103/PhysRevB.77.024112.
11. Belozerov, V., Sobol O., Mahatilova A., Subbotina V., Tabaza T. A., Al-Qawabeha U. F., Al-Qawabah S. M. The influence of the conditions of microplasma processing (microarc oxidation in anode-cathode regime) of aluminum alloys on their phase composition. *Eastern-European journal of enterprise technologies*. 2017. 5. Iss. 12–89. P. 52–57. doi: 10.15587/1729-4061.2017.112065.
12. Rudolph M., Motylenko M., Rafaja D. Structure model of γ-Al_2O_3 based on planar defects. *IUCrJ*. 2019. 6. Iss. 1. P. 116–127. doi.10.1107/S2052252518015786.
13. Rudolph M., Salomon A., Schmidt A., Motylenko M., Zienert T., Stöcker H., Himcinschi C., Amirkhanyan L., Kortus J., Aneziris C. G., Rafaja D. Thermally induced formation of transition aluminas from boehmite. *Advanced Engineering Materials*. 2017. 19. Iss. 9. P. 1700141. doi.10.1002/adem.201700141.
14. Pakharukova V., Yatsenko D., Gerasimov E. Y., Shalygin A., Martyanov O., Tsybulya S. Coherent 3D Nanostructure of γ-Al2O3: Simulation of whole X-ray powder diffraction pattern. *Journal of solid state chemistry*. 2017. 246. P. 284–292. doi.10.1016/j.jssc.2016.11.032.
15. Navrotsky A. Energetics of nanoparticle oxides: interplay between surface energy and polymorphism. *Geochemical transactions*. 2003. 4. № 6. P. 34–37. doi: 10.1186/1467-4866-4-34.
16. Castro R. H. R., Ushakov S. V., Gengembre L., Gouvêa D., and Navrotsky A. Surface energy and thermodynamic stability of γ-alumina: effect of dopants and water. *Chemistry of materials*. 2006. 18. Iss. 7. P. 1867–1872. doi: 10.1021/cm052599d.
17. Wriedt H. A. The Al-O (Aluminum-Oxygen) system. *Bulletin of Alloy Phase Diagrams*. 1985. 6. P. 548–553.
18. Xu Y. N., Ching W. Y. Self-consistent band structures, charge distributions, and optical-absorption spectra in MgO, alpha-Al_2O_3, and $MgAl_2O_4$. *Journal physical review B*. 1991. 43. Iss. 5. P. 4461–4472. doi: 10.1103/physrevb.43.4461.
19. Clyne T. W., Troughton S. C. A review of recent work on discharge characteristics during plasma electrolytic oxidation of various metals. *International materials reviews*. 2018. 64. Iss. 3. P. 127–162. doi: 10.1080/09506608.2018.1466492.
20. Решетняк М. В., Соболь О. В. Расширение возможностей анализа структуры и субструктурных

характеристик нанокристаллических конденсированных и массивных материалов квазибинарной системы W_2B_5-TiB_2 при использовании программы обработки рентгендифракционных данных «new_profile». *Фізична інженерія поверхні*. 2008. Т. 6. № 3–4. С. 180–188.

21. Toby B. H., Harlow R. L., Hohmany M. A. The powder suite: Computer Programs for Searching and Accessing the TCPDS-ICDD Powder Diffraction Database. *Powder Diffraction.* 1990. 5. Iss. 1. P. 2–7. doi: 10.1017/S0885715600015153.
22. McHale J. M., Auroux A., Perrota A. J., Navrotsky A., Surface Energies and thermodynamic phase stability in nanocrystalline aluminas. *Science*. 1997. 277. Iss. 5327. P. 788–791. doi: 10.1126/science.277.5327.788.
23. Trueba M., Trasatti S. P. γ-Alumina as a support for catalysts: a review of fundamental aspects. *European journal of inorganic chemistry*. 2005. 2005. № 17. P. 3393–3403. doi: 10.1002/ejic.200500348.
24. Zhou R. S., Snyder R. L. Structures and transformation mechanisms of the η, γ and θ transition aluminas. *Acta crystallographica Section B.* 1991. 47. Iss. 5. P. 617–630. doi: 10.1107/S0108768191002719.
25. Wilson S. J., Mc Connell J. D. C. A kinetic study of the system γ-AlOOHAl_2O_3. *Journal of solid state chemistry*. 1980. 34. Iss. 3. P. 315–322. doi: 10.1016/0022-4596(80)90429-6.
26. Paglia G., Buckley C. E., Rohl A. L., Hart R. D., Winter K., Studer A. J., Hunter B. A., Hanna J. V. Boehmite derived γ-alumina system. 1. Structural evolution with temperature, with the identification and structural determination of a new transition phase, γ′-alumina. *Chemistry of materials*. 2004. 16. Iss. 2. P. 220–236. doi: 10.1021/cm034917j.
27. Paglia G., Buckley C. E., Rohl A. L., Hunter B. A. Hart R. D., Hanna J. V., Byrne L. T. Tetragonal structure model for boehmite-derived γ-alumina. *Physical review. B*. 2003. 68, Iss. 14. P. 144110.1–11. doi: 10.1103/PhysRevB.68.144110.
28. Loyola C., Menendez-Proupin E., Gutierrez G., Atomistic study of vibrational properties of γ-Al_2O_3. *Journal of materials science*. 2010. 45. P. 5094–5100. doi: 10.1007/s10853-010-4477-5.
29. Prins R. Location of the spinel vacancies in γ-Al_2O_3. *Angewandte chemie*. 2019. 131. Iss. 43. P. 15694–15698. doi: 10.1002/ange.201901497.
30. Wolverton C., Hass K. C., Phase stability and structure of spinel-based transition aluminas. *Physical review B*. 2001. 63. Iss. 2. P. 024102-1–16. doi: 10.1103/PhysRevB.63.024102.
31. Gutierrez G., Taga A., Johansson B. Theoretical structure determination of γ-Al_2O_3. *Physical review B*. 2001. 65. Iss. 1. P. 012101-1–4. doi: 10.1103/PhysRevB.65.012101.
32. Cai S. H., Rashkeev S. N., Pantelides S. T., Sohlberg K. Atomic scale mechanism of the transformation of γ-alumina to θ-alumina. *Physical review letters*. 2002. 89. Iss. 23. P. 235501-1–4. doi: 10.1103/ PhysRevLett.89.235501.
33. Cai S. H., Rashkeev S. N., Pantelides S. T., Sohlberg K. Phase transformation mechanism between gamma- and theta-alumina. *Physical review B.* 2003. 67. Iss. 22. P. 224104-1–10. doi:10.1103/PhysRevB.67.224104.
34. Pinto H. P., Nieminen R. M., Elliott S. D. Ab initio study of Al_2O_3 surfaces. *Physical review B.* 2004. 70. Iss. 12. P. 125402-1–11. doi: 10.1103/PhysRevB.70.125402.
35. Menendez-Proupin E., Guti.errez G., Electronic properties of bulk γ-Al_2O_3. *Physical review B.* 2005. 72. P. 035116-1–9. doi: 10.1103/PhysRevB.72.035116.
36. Гусев А. И. *Нестехиометрия, беспорядок, ближний и дальний порядок в твердом теле*. М.: ФИЗМАТЛИТ, 2007. 856 с.
37. Yoshitake M., Bera S., Yamuchi Y., Song W. The growth of well-ordered ultra-thin Al_2O_3 films on Cu-Al alloy. *Hyomen Kagaku.* 2003. 24. № 7. P. 438–440. doi: 10.1380/jsssj.24.438.

References (transliterated)

1. Xiang N., Song R.-g., Zhuang J.-j. Song R.-x., Lu X.-y., Su X.-p. Effects of current density on microstructure and properties of plasma electrolytic oxidation ceramic coatings formed on 6063 aluminum alloy. *Transactions of nonferrous metals society of china*, 2016, 26, Iss. 3, pp. 806–813, doi: 10.1016/S1003-6326(16)64171-7.
2. Kharanagh V. J., Sani M. AF., Rafizadeh E. Effect of current frequency on coating properties formed on aluminized steel by plasma electrolytic oxidation. *Surface engineering*, 2014, 30, Iss. 3, pp. 224–228, doi: 10.1179/1743294413Y.0000000190.
3. Martin J., Melhem A., Shchedrina I., Duchanoy T., Nominé A., Henrion G., Czerwiec T., Belmonte T. Effects of electrical parameters on plasma electrolytic oxidation of aluminium. *Surface and coatings technology*, 2013, 221, pp. 70–76, doi: 10.1016/j.surfcoat.2013.01.029.
4. Lesnevskiy L. N., Lyakhovetskiy M. A., Ivanova S. V., Nagovitsyna O. A. Structure and properties of surface layers formed on zirconium alloy by microarc oxidation. *Journal of surface investigation. X-ray, synchrotron and neutron techniques*, 2016, 10, Iss. 3, pp. 641–647, doi: 10.1134/S1027451016030289.
5. Li H. X., Li W. J., Song R. G., Ji Z. Effects of different current densities on properties of MAO coatings embedded with and without a-Al_2O_3 nanoadditives. *Materials science and technology*, 2012, 28, Iss. 5, pp. 565–568, doi: 10.1179/1743284711Y.0000000084.
6. Veys-Renaux D., Rocca E., Henrion G. Micro-arc oxidation of AZ91 Mg alloy: An in-situ electrochemical study. *Electrochemistry communications*, 2013, 31, pp. 42–45, doi: 10.1016/j.elecom.2013.02.023.
7. Subbotina V., Al-Qawabeha U. F., Belozerov V., Sobol' O., Subbotin A., Tabaza T. A., Al-Qawabah S. M. Determination of influence of electrolyte composition and impurities on the content of α-Al_2O_3 phase in mao-coatings on aluminum. *Eastern-european journal of enterprise technologies*, 2019, 6, Iss. 12 (102), pp. 6–13, doi: 10.15587/1729-4061.2019.185674.
8. Belozerov V., Mahatilova A., Sobol' O., Subbotina, V., Subbotin A. Investigation of the influence of technological conditions of microarc oxidation of magnesium alloys on their structural state and mechanical properties. *Eastern-European journal of enterprise technologies*, 2017, 2, Iss. 5 (86), pp. 39–43, doi: 10.15587/1729-4061.2017.96721.
9. Bron V. A. O rekristallizatsii korunda [About recrystallization of corundum]. *Dokladyi Akademii Nauk SSSR*, 1951, 80, no. 4, pp. 661–664.
10. Tsybulya S. V. Kryukova G.N. Nanocrystalline transition aluminas: Nanostructure and features of x-ray powder diffraction patterns of low-temperature Al_2O_3 polymorphs. *Physical Review B*, 2008, 77, Iss. 2, pp. 024112, doi:10.1103/PhysRevB.77.024112.
11. Belozerov, V., Sobol O., Mahatilova A., Subbotina V., Tabaza T. A., Al-Qawabeha U. F., Al-Qawabah S. M. The influence of the conditions of microplasma processing (microarc oxidation in anode-cathode regime) of aluminum

ISSN 2079-5459 (print)
ISSN 2413-4295 (online)

alloys on their phase composition. *Eastern-European journal of enterprise technologies*, 2017, 5, Iss. 12–89, pp. 52–57, doi: 10.15587/1729-4061.2017.112065.
12. Rudolph M., Motylenko M., Rafaja D. Structure model of γ-Al_2O_3 based on planar defects. *IUCrJ,* 2019, 6, Iss. 1, pp. 116–127, doi: 10.1107/S2052252518015786.
13. Rudolph M., Salomon A., Schmidt A., Motylenko M., Zienert T., Stöcker H., Himcinschi C., Amirkhanyan L., Kortus J., Aneziris C. G. & Rafaja D. Thermally induced formation of transition aluminas from boehmite. *Advanced Engineering Materials,* 2017, 19, Iss. 9, p. 1700141, doi: 10.1002/adem.201700141.
14. Pakharukova V., Yatsenko D., Gerasimov E. Y., Shalygin A., Martyanov O. & Tsybulya S. Coherent 3D Nanostructure of γ-Al2O3: Simulation of whole X-ray powder diffraction pattern. *Journal of solid state chemistry,* 2017, 246, pp. 284–292, doi: 10.1016/j.jssc.2016.11.032.
15. Navrotsky A. Energetics of nanoparticle oxides: interplay between surface energy and polymorphism. *Geochemical transactions*, 2003, 4, no. 6, pp. 34–37, doi: 10.1186/1467-4866-4-34.
16. Castro R. H. R., Ushakov S. V., Gengembre L., Gouvêa D., and Navrotsky A. Surface energy and thermodynamic stability of γ-alumina: effect of dopants and water. *Chemistry of materials*, 2006, 18, Iss. 7, pp. 1867–1872, doi: 10.1021/cm052599d.
17. Wriedt H. A. The Al-O (Aluminum-Oxygen) system. *Bulletin of Alloy Phase Diagrams*, 1985, 6, pp. 548–553.
18. Xu Y. N., Ching W. Y. Self-consistent band structures, charge distributions, and optical-absorption spectra in MgO, alpha-Al_2O_3, and $MgAl_2O_4$. *Journal physical review B*, 1991, 43, Iss. 5, pp. 4461–4472, doi: 10.1103/physrevb.43.4461.
19. Clyne T. W., Troughton S. C. A review of recent work on discharge characteristics during plasma electrolytic oxidation of various metals. *International materials reviews*, 2018, 64, Iss. 3, pp. 127–162, doi: 10.1080/09506608.2018.1466492.
20. Reshetnyak M. V., Sobol O. V. Rasshirenie vozmozhnostey analiza strukturyi i substrukturnyih harakteristik nanokristallicheskih kondensirovannyih i massivnyih materialov kvazibinarnoy sistemyi W2B5-TiB2 pri ispolzovanii programmyi obrabotki rentgendifraktsionnyih dannyih «new_profile» [Expanding the capabilities of analyzing the structure and substructural characteristics of nanocrystalline condensed and massive materials of the quasi-binary system W2B5-TiB2 using the X-ray diffraction data processing program "new_profile"]. *FIzichna inzheneriya poverhni*, 2008, 6, no. 3–4, pp. 180–188.
21. Toby B. H., Harlow R. L., Hohmany M. A. The powder suite: Computer Programs for Searching and Accessing the TCPDS-ICDD Powder Diffraction Database. *Powder Diffraction*, 1990, 5, Iss. 1, pp. 2–7. doi: 10.1017/S0885715600015153.
22. McHale J. M., Auroux A., Perrota A. J., Navrotsky A., Surface energies and thermodynamic phase stability in nanocrystalline aluminas. *Science*, 1997, 277, Iss. 5327, pp. 788–791, doi: 10.1126/science.277.5327.788.
23. Trueba M., Trasatti S. P. γ-Alumina as a support for catalysts: a review of fundamental aspects. *European journal of inorganic chemistry*, 2005, 2005, № 17, pp. 3393–3403, doi: 10.1002/ejic.200500348.
24. Zhou R. S., Snyder R. L. Structures and transformation mechanisms of the η, γ and θ transition aluminas. *Acta crystallographica Section B*, 1991, 47, Iss. 5, pp. 617–630. doi: 10.1107/S0108768191002719.
25. Wilson S. J., Mc Connell J. D. C. A kinetic study of the system γ-AlOOHAl_2O_3. *Journal of solid state chemistry*, 1980, 34, Iss. 3, pp. 315–322, doi: 10.1016/0022-4596(80)90429-6.
26. Paglia G., Buckley C. E., Rohl A. L., Hart R. D., Winter K., Studer A. J., Hunter B. A., Hanna J. V. Boehmite derived γ-alumina system. 1. Structural evolution with temperature, with the identification and structural determination of a new transition phase, γ′-alumina. *Chemistry of materials,* 2004, 16, Iss. 2, pp. 220–236. doi: 10.1021/cm034917j.
27. Paglia G., Buckley C. E., Rohl A. L., Hunter B. A., Hart R. D., Hanna J. V., Byrne L. T. Tetragonal structure model for boehmite-derived γ-alumina. *Physical review. B,* 2003, 68, Iss. 14, pp. 144110.1–11, doi: 10.1103/PhysRevB.68.144110.
28. Loyola C., Menendez-Proupin E., Gutierrez G., Atomistic study of vibrational properties of γ-Al_2O_3. *Journal of materials science*, 2010, 45, pp. 5094–5100, doi: 10.1007/s10853-010-4477-5.
29. Prins R. Location of the spinel vacancies in γ-Al_2O_3. *Angewandte chemie*, 2019, 131, Iss. 43, pp. 15694–15698, doi: 10.1002/ange.201901497.
30. Wolverton C., Hass K. C. Phase stability and structure of spinel-based transition aluminas. *Physical review B*, 2001, 63, Iss. 2, pp. 024102-1–16. doi: 10.1103/PhysRevB.63.024102.
31. Gutierrez G., Taga A., Johansson B. Theoretical structure determination of γ-Al_2O_3. *Physical Review B*, 2001, 65, Iss. 1. pp. 012101-1–4, doi: 10.1103/PhysRevB.65.012101.
32. Cai S. H., Rashkeev S. N., Pantelides S. T., Sohlberg K. Atomic scale mechanism of the transformation of γ-alumina to θ-alumina. *Physical review letters*, 2002, 89, Iss. 23, pp. 235501-1–4. doi: 10.1103/PhysRevLett.89.235501.
33. Cai S. H., Rashkeev S. N., Pantelides S. T., Sohlberg K. Phase transformation mechanism between gamma- and theta-alumina. *Physical review B,* 2003, 67, Iss. 22, pp. 224104-1–10, doi: 10.1103/PhysRevB.67.224104.
34. Pinto H. P., Nieminen R. M., Elliott S. D. Ab initio study of Al_2O_3 surfaces. *Physical review B.* 2004. 70, Iss. 12, pp. 125402-1–11, doi: 10.1103/PhysRevB.70.125402.
35. Menendez-Proupin E., Guti.errez G., Electronic properties of bulk γ-Al_2O_3. *Physical review B.,* 2005, 72, pp. 035116-1–9, doi: 10.1103/PhysRevB.72.035116.
36. Gusev A. I. *Nestehiometriya, besporyadok, blizhniy i dalniy poryadok v tverdom tele [Nonstoichiometry, disorder, short-range and long-range order in a solid body]*. M., FIZMATLIT, 2007. 856 p.
37. Yoshitake M., Bera S., Yamuchi Y., Song W. The growth of well-ordered ultra-thin Al_2O_3 films on Cu-Al alloy. *Hyomen Kagaku*, ·2003, 24, no. 7, pp. 438–440, doi: 10.1380/jsssj.24.438.

Відомості про авторів (About authors)

Oleg Sobol – Doctor of Physics and Mathematics sciences, professor, National Technical University «Kharkiv Polytechnic Institute», professor at the department of materials science, Kharkiv, Ukraine; ORCID: 0000-0002-4497-4419; e-mail: sool@kpi.kharkov.ua

Соболь Олег Валентинович – доктор фізико-математичних наук, професор, Національний технічний університет

«Харківський політехнічний інститут» професор кафедри матеріалознавства, м. Харків, Україна; ORCID: 0000-0002-4497-4419; e-mail: sool@kpi.kharkov.ua

Valeria Subbotina – PhD, National Technical University «Kharkiv Polytechnic Institute», associate professor at the department of materials science, Kharkiv, Ukraine; ORCID: 0000-0002-3882-0368; e-mail: subbotina.valeri@gmail.com

Субботіна Валерія Валеріївна – кандидат технічних наук, Національний технічний університет «Харківський політехнічний інститут», доцент кафедри матеріалознавства, м. Харків, Україна; ORCID: 0000-0002-3882-0368; e-mail: subbotina.valeri@gmail.com

Please cite this article as:

Sobol' O., Subbotina V. Regularities of the influence of microarc oxidation of aluminum alloys on the phase-structural state of the formed oxide coatings and the peculiarities of γ-AL_2O_3 → α-AL_2O_3 polymorphic transformation during their annealing. *Bulletin of the National Technical University "KhPI". Series: New solutions in modern technology*. – Kharkiv: NTU "KhPI", 2020, no. 3 (5), pp. 10–21, doi:10.20998/2413-4295.2020.01.02.

Будь ласка, посилайтесь на цю статтю наступним чином:

Соболь О. В., Субботіна В. В. Закономірності впливу мікродугового оксидування алюмінієвих сплавів на фазово-структурний стан формованих оксидних покриттів і особливості γ-Al_2O_3 →α-Al_2O_3 поліморфного перетворення при їх відпалі. *Вісник Національного технічного університету «ХПІ». Серія: Нові рішення в сучасних технологіях*. – Харків: НТУ «ХПІ». 2020. № 3 (5). С. 10–21. doi:10.20998/2413-4295.2020.01.02.

Пожалуйста, ссылайтесь на эту статью следующим образом:

Соболь О. В., Субботина В. В. Закономерности влияния микродугового оксидирования алюминиевых сплавов на фазово-структурное состояние формируемых оксидных покрытий и особенности γ-Al_2O_3 →α-Al_2O_3 полиморфного превращения при их отжиге. *Вестник Национального технического университета «ХПИ». Серия: Новые решения в современных технологиях*. – Харьков: НТУ «ХПИ». 2020. № 3 (5). С. 10–21. doi:10.20998/2413-4295.2020.01.02.

АННОТАЦИЯ *Изучено влияние технологических параметров микродугового оксидирования на закономерности фазово-структурного состояния покрытий, формируемых на алюминиевых сплавах Д16 (основной элемент легирования Cu) и АМг (основной элемент легирования Mg) и влияние отжигов в интервале температур 600–1280 °С на фазовое превращение γ-Al_2O_3 → α-Al_2O_3. Установлено, что в покрытиях, формируемых при микродуговом оксидировании в комплексном (щелочно-силикатном) электролите, выявляются три основные фазово-структурные состояния: γ-Al_2O_3, α-Al_2O_3 и муллит ($3Al_2O_3$•$2SiO_2$). Определены условия электролиза позволяющие формироваться двухфазному состоянию (γ-Al_2O_3 и α-Al_2O_3) на сплавах обоих типов. 4. Установлено, что легирующие элементы сплава АМг3 обеспечивают в МДО-покрытиях более высокую стабильность структуры γ-A12O3, по сравнению с аналогичным состоянием в МДО-покрытиях на сплаве Д16 Высокотемпературный отжиг МДО-покрытий позволил выявить более полное фазовое превращение на сплаве Д16 структкрной основой которого является появление тетрагональности в дефектной кубической решетки γ-Al_2O_3 фазы. Отжиг МДО-покрытий стимулирует γ → α превращение с наибольшей динамикой изменения в покрытиях, полученных на сплаве Д16. При наибольшей температуре отжига 1280 °С (в течение 60 мин.) в результате γ → α превращения относительное содержание α-Al2O3 фазы в покрытии составляет 89 % (покрытие, полученное на сплаве Д16) и 30% (покрытие, полученное на сплаве АМг3). Предложена модель полиморфного γ-Al_2O_3 → α-Al_2O_3 превращения в оксиде алюминия, основанная на упорядочении металлической катионной подсистемы в октаэдрических и тетраэдрических междоузлиях и усиление этого процесса при ослаблении связи «металл–кислород» в результате замещения ионов Al ионами Cu, имеющими низкую энергию связи с кислородом. Выявлена корреляция между относительным содержанием α-Al2O3 фазы и твердостью МДО-покрытия. При наибольшем содержании α-Al2O3 фазы твердость достигает 16000 МПа.*

Ключевые слова: *микродуговое оксидирование; алюминиевый сплав; щелочно силикатный электролит; γ-Al_2O_3; элементы легирования; отжиг; междоузлиях; тетрагональность; полиморфное превращение*

Received 02.09.2020